


## Article

# UV-Curable Silicone-Modified Polyurethane Acrylates for Food Freshness Monitoring

Na He <sup>1</sup>, Hongyu Zhu <sup>1</sup>, Nana Sun <sup>1</sup>, Shaoqing Shi <sup>2</sup>, Libo Xie <sup>2</sup>, Jie Miao <sup>2</sup>, Guoqiao Lai <sup>1,\*</sup>, Meijiang Li <sup>1,\*</sup> and Xiongfa Yang <sup>1,\*</sup> 

<sup>1</sup> College of Material, Chemistry and Chemical Engineering, Key Laboratory of Organosilicon Chemistry and Material Technology of Ministry of Education, Key Laboratory of Silicone Materials Technology of Zhejiang Province, Hangzhou Normal University, Hangzhou 311121, China; hena@stu.hznu.edu.cn (N.H.); 2022112009067@stu.hznu.edu.cn (H.Z.); 2022112009005@stu.hznu.edu.cn (N.S.)

<sup>2</sup> Yuyao Yuandong Chemical Co., Ltd., Yuyao 315403, China; yyydhg@163.com (S.S.); 13606594866@163.com (L.X.); yuandongmiaojie@163.com (J.M.)

\* Correspondence: laiguogiao@aliyun.com (G.L.); limeijiang@hznu.com (M.L.); yangxiongfa@hznu.edu.cn (X.Y.)

**Abstract:** Intelligent materials for monitoring the condition of the packaged food or its surroundings are highly desired to ensure food safety. In this paper, UV-curable silicone-modified materials for monitoring the freshness of high-protein food such as shrimp and pork were prepared from polyurethane acrylates with covalent-grafted neutral red groups and thiol silicone resin. The UV-curable materials exhibited visible pH-sensitive performance and long-term color stability because their color did not change when they were immersed in aqueous solutions with different pH values for 20 min, and the color remained even when they were immersed for over 5 h. The distinctive color variation in the UV coatings makes them suitable as potential pH-sensitive sensors. These pH-sensitive intelligent materials can be applied to monitor the freshness of high-protein food such as shrimp and pork. Additionally, the thermal stability and adhesive properties of the UV-curable materials were also studied. A conclusion can be drawn that the covalent bonding of neutral red groups onto a silicone-modified polymer matrix is an ideal strategy for developing pH-sensitive intelligent materials with good pH stability for monitoring the freshness of high-protein food.

**Keywords:** pH-sensitive intelligent materials; food freshness monitoring; UV curable; silicone-modified materials



**Citation:** He, N.; Zhu, H.; Sun, N.; Shi, S.; Xie, L.; Miao, J.; Lai, G.; Li, M.; Yang, X. UV-Curable Silicone-Modified Polyurethane Acrylates for Food Freshness Monitoring. *Coatings* **2024**, *14*, 728. <https://doi.org/10.3390/coatings14060728>

Academic Editor: Muhammad Ahsan Bashir

Received: 27 April 2024

Revised: 26 May 2024

Accepted: 4 June 2024

Published: 6 June 2024



**Copyright:** © 2024 by the authors. Licensee MDPI, Basel, Switzerland. This article is an open access article distributed under the terms and conditions of the Creative Commons Attribution (CC BY) license (<https://creativecommons.org/licenses/by/4.0/>).

## 1. Introduction

Animal-derived foods such as shrimp and pork are widely consumed because of their superior nutritional composition. However, in the fabrication and sale chain, these foods can produce some substances that are harmful to human beings such as aldehydes, acids, amines, ammonia, hydrogen sulfide, phenol, mercaptans, etc. [1,2]. So, intelligent materials are highly desired for monitoring quality information to ensure food safety [3–7]. Recently, Sangeetha et al. prepared an intelligent packaging material from coconut husk-lignin-derived carbon dots and carrageenan [8]. Yue et al. prepared an intelligent packaging film with antibacterial performance using cellulose fibers, cellulose nanofibers, ZnO nanoparticles, and polydiacetylene [9]. Ronte et al. developed intelligent packaging material using chitosan grafted with phenol red to monitor shrimp freshness by pH changes [10]. The pH change in food attributed to amino acids and glucose metabolism is one of the important and effective parameters for identifying food spoilage [11]. Low molecular synthetic pH indicators are not suitable for monitoring food spoilage because of their toxic, carcinogenic, and mutagenic properties. Natural dyes such as anthocyanins, curcumin, alizarin, and betalains, with safe, non-toxicity, and renewability properties, are ideal sources of pH indicator materials [12–14]. However, the poor stability and insensitivity to minor changes

in pH for natural pH indicators exposed to different environmental conditions seriously limit their applications [15,16].

To reduce toxicity and improve the stability of pH-sensitive intelligent materials, the covalent bonding of pH indicator groups onto a polymer matrix is a reliable strategy because the release probability of the dyes is greatly reduced. For example, a membrane with a visible color change at different pH conditions of 2–12 was developed by immobilizing pH-sensitive dyes onto ethyl cellulose nanofibers, which exhibited good stability for up to 7 days at room temperature [17]. A pH-sensitive material for monitoring the freshness of pork for 12 days was also fabricated by the covalent grafting of oregano essential oil and black rice bran anthocyanin onto a chitosan matrix [18]. Neutral red (NR), an easily available water-soluble, pH-sensitive dye in the pH value range of 4–6 with relatively low toxicity, has been widely used [19]. Khanjanzadeh et al. [20] developed pH-sensitive films with visible color variation at a pH value of 2–10 by covalent bonding NR onto cellulose nanofibrils. Their work revealed that NR is a good candidate for covalent bonding onto a polymer matrix to develop pH-sensitive intelligent materials.

UV-cured technology has gained much attention in the coating industry because of its high efficiency, environmentally friendly, and energy-saving merits [21]. The outstanding performance of UV-curable silicone-modified materials such as non-toxicity and excellent chemical and thermal stability makes them broadly used in electronics, sensors, and coatings [22,23]. In this paper, UV-curable pH-sensitive intelligent silicone-modified coatings for monitoring the freshness of high-protein food such as shrimp and pork were prepared. The materials have a good pH-sensitive property and long-term color stability, which have potential usages in monitoring the freshness of high-protein food.

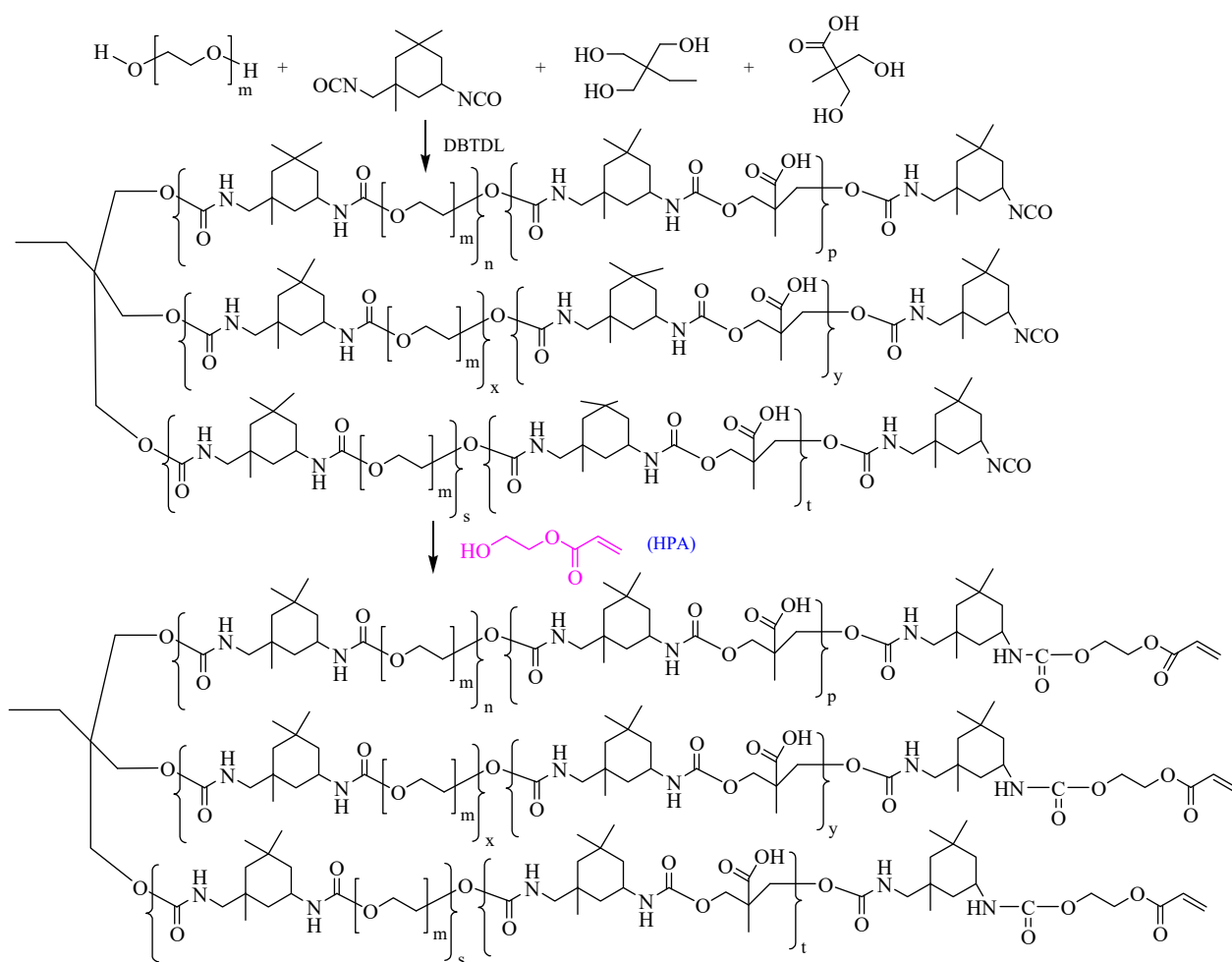
## 2. Materials and Methods

### 2.1. Materials

Isophorone diisocyanate (IPDI, 98%, mixture of isomers) and acetone (A. R.) were supplied by Sinopharm Chemical Reagent Co., Ltd. (Shanghai, China). Poly(ethylene glycol) (average Mn ~600, PEG-600), N-hydroxy succinimide (NHS, A. R.), and 1-(3-dimethylaminopropyl)-3-ethylcarbodiimide hydrochloride (EDC, A. R.) were bought from Shanghai McLean Biochemical Technology Co., Ltd. (Shanghai, China). Neutral red (NR, A. R.) was purchased from Shanghai Yuanye Biotechnology Co., Ltd. (Shanghai, China). Dimethyldimethoxysilane (A. R.) and methyltrimethoxysilane (A. R.) were supplied by Shanghai Jiancheng Industry and Trade Co., Ltd. (Shanghai, China). Mercaptopropyltrimethoxysilane (A. R.), 2-hydroxy-1-methylethyl acrylate (HMA, A. R.), dibutyltin dilaurate (DBTDL, A. R.), dimethylolbutanoic acid (DMBA, A. R.), and trimethylolpropane (TMP, A. R.) were bought from Beijing HWRK Chem Co., Ltd. (Beijing, China). Hydrochloric acid (A. R., 36.5%) and toluene (A. R.) were bought from Hangzhou Shuanglin Chemical Reagent Co., Ltd. (Hangzhou, China). 2-Hydroxy-2-methyl-1-phenylacetone (HMPP, 99.0%, AR) was obtained from Shanghai Qitai Chemical Technology Co., Ltd. (Shanghai, China). Except for thiol silicone resin with a thiol content of 4 mmol g<sup>-1</sup>, which was prepared according to references [22–24], the other chemical reagents were purchased and used as received.

### 2.2. Preparation of NR Covalent-Grafted Polyurethane Acrylates (NR-PUAs)

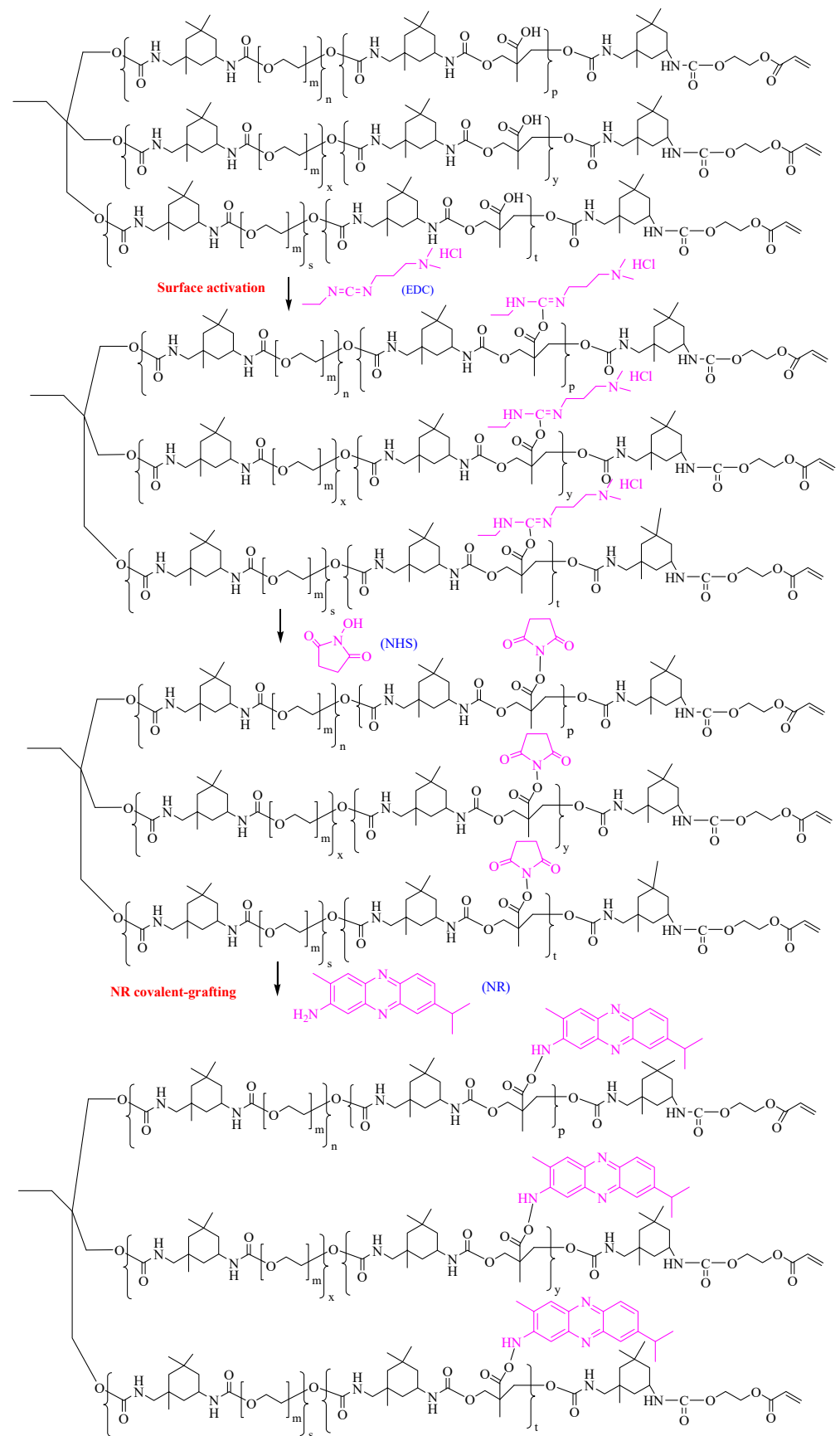
Several polyurethane acrylates (PUAs) (Scheme 1) were prepared according to reference [19] by the formula shown in Table S1. For example, 0.3704 g DMBA, 28.5 g PEG-600, 0.4025 g TMP, 0.2168 g DBTDL, and 54.2 g acetone were mixed homogeneously, then 24.937 g IPDI was dropped in at 40 °C for 1 h, and the reaction was carried out at 60 °C for about 2 h. After that, 14.185 g HPA was added, and the reaction was conducted for another 2 h at 60 °C. Finally, a transparent sticky liquid of PUA-1 was prepared after being distilled at 130 mmHg/50 °C for about 1 h to remove acetone.



**Scheme 1.** Procedure for the preparation of PUAs.

Consequently, several NR-PUAs were fabricated according to reference [18], following the procedure shown in Scheme 2 and the formula shown in Table S2. For example, 0.0690 g EDC·HCl in 0.0276 g THF and 0.1104 g ethanol was added into a mixture of 10.0 g PUA-1, 4.0 g THF, and 16.0 g ethanol at 55 °C for 1 h, and the reaction was carried out for another 2 h. Then, 0.0420 g NHS in 0.0168 g THF and 0.0672 g ethanol was added at 0–5 °C for 0.5 h. The reaction was conducted for another 1 h. Later, 0.1050 g NR in 0.0420 g THF and 0.1680 g ethanol was added, and the reaction was conducted for about 24 h. Before the NR-PUA-1 product was obtained, the mixture was filtered with medium-speed filter paper to remove residual solid NR and distilled at 130 mmHg/60 °C for about 2 h to remove solvents.

Fourier transform infrared (FT-IR) spectrum analysis of NR-PUA-3 was adopted to characterize the NR-PUAs (Figure 1). The sharp, moderate, single absorption peak at about 3335 cm<sup>-1</sup>, rather than a double absorption peak, is the characteristic stretching vibration of N-H groups of NR [25]. The absorption peak at about 1703 cm<sup>-1</sup> is attributed to the amide bond resulting from the interaction between the carboxyl groups and the amino groups of NR. The peaks at about 2932 cm<sup>-1</sup> and 1621 cm<sup>-1</sup> are the characteristic absorption of C=C in acrylate groups. So, it can be concluded that NR was grafted onto the PUAs.



**Scheme 2.** Procedure for the preparation of NR-PUAs.

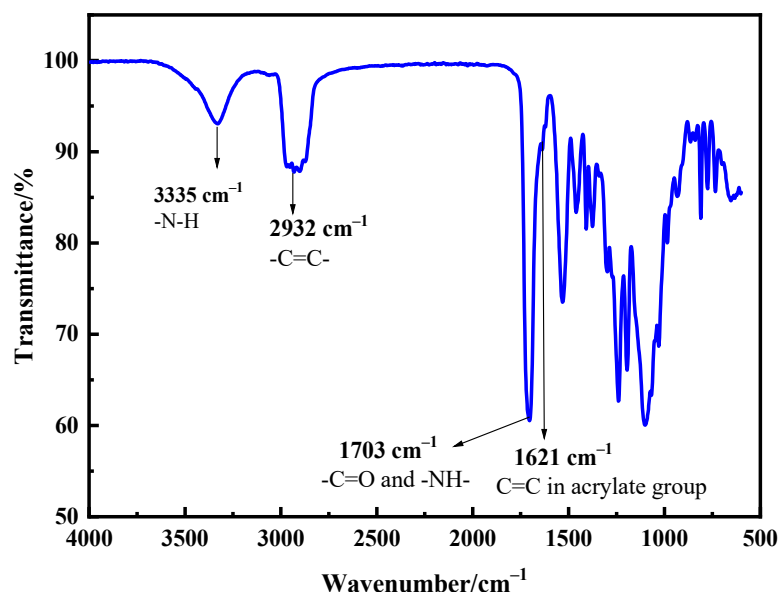
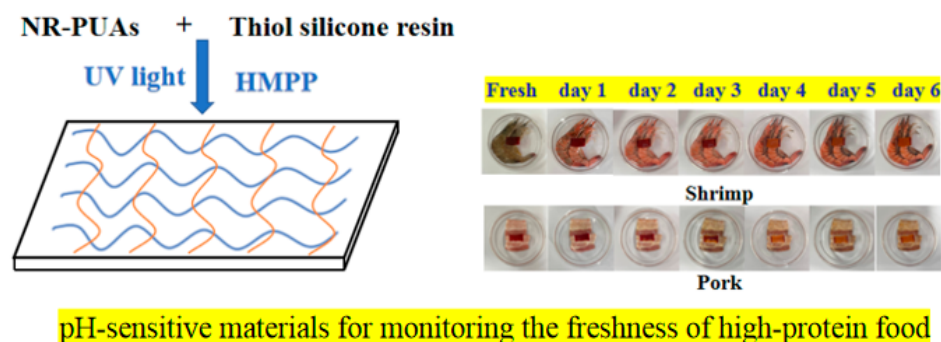


Figure 1. FT-IR spectrum of NR-PUA-3.

### 2.3. Fabrication of UV-Curable Silicone-Modified Coatings (UV Coatings)

As exhibited in Scheme 3, UV coatings (thickness of about 0.3 mm) were prepared from NR-PUAs, thiol silicone resin, and 3 wt% HMPP by UV (ZB1000, Changzhou Zibo Electron Technology Co., Ltd., Changzhou, China; laser wavelength of 365 nm, radiation intensity of  $10.6 \text{ mW} \cdot \text{cm}^{-2}$ , and a distance of the slides to the light of 20 cm).



pH-sensitive materials for monitoring the freshness of high-protein food

Scheme 3. Fabrication of the UV coatings.

### 2.4. Characterization

<sup>1</sup>H NMR spectra were conducted on a Bruker AVANCE AV400 (400 MHz) spectrometer (Bruker Corporation, Karlsruhe, Germany) in CDCl<sub>3</sub>. FT-IR analysis was carried out using a Nicolet 700 spectrometer (Nicolet Co., Ltd., Madison, WI, USA). The pencil hardness, gel-sol fraction, adhesion property, cross-linking density (SD), and thermogravimetric analysis (TGA) of the UV coatings were measured according to reference [22,26]. Differential Scanning calorimeter (DSC) analysis was carried out on a DSC Q100 apparatus (TA Instruments, New Castle, DE, USA) under N<sub>2</sub> atmosphere with a flow rate of  $10 \text{ mL min}^{-1}$ . The coating samples were heated from room temperature to 80 °C and held for 2 min to erase the thermal history, cooled to -30 °C at a rate of  $10 \text{ °C min}^{-1}$ , and finally heated again to 80 °C at a heating rate of  $10 \text{ °C min}^{-1}$ . The color variation was recorded by Na He using a mobile phone (iPhone XS Max, Apple, Cupertino, CA, USA) after the coatings on the glass slides were immersed in the aqueous with different pH values for about 20 min. Monitoring of the freshness of shrimp and pork was conducted as follows: The shrimp and pork were put into separate culture dishes, and a piece of crimson film peeled off from the UV-curable, silicone-modified coating was pasted inside the top cover of each culture dish.

Then, the experiment for monitoring the freshness of shrimp and pork was carried out at 25 °C.

### 3. Results and Discussion

#### 3.1. Preparation of UV COATINGS

##### 3.1.1. Impact of UV Curing Time

The impact of UV curing time is summarized in Table 1. The gel–sol fraction and the pencil hardness of the UV coatings increased continuously from 57.3% to 89.4% and 6 B to H, respectively. When the curing time was >50 s, both the curing content and the pencil hardness were affected slightly by the prolongation of curing time. These coatings were analyzed by FT–IR, as shown in Figure 2. It can be noticed that the characteristic peaks of C=C in acrylate groups at 1610  $\text{cm}^{-1}$  disappeared when the UV curing time was about 30–50 s. So, 50 s was selected as a suitable UV curing time.

**Table 1.** Impact of UV curing time on the performance of UV-curable coatings.

Curing Time/s	Gel–Sol Fraction/wt%	Pencil Hardness
20	57.3	6B
30	75.7	4B
40	80.3	B
50	89.4	H
60	89.8	H

Conditions: NR–PUA is NR–PUA–3. The molar ratio of acrylate groups to thiol groups ( $n_{\text{acrylate}}:n_{\text{thiol}}$ ) is 1:1, and the amount of HMPP is 3% of the total mass of NR–PUA–3 and thiol resin.

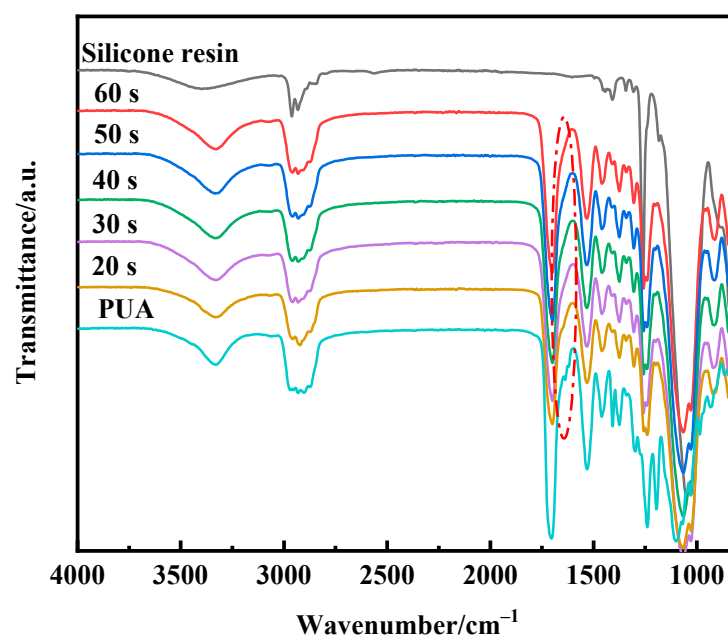


**Figure 2.** FT–IR spectra of UV coatings prepared at different times.

##### 3.1.2. Impact of Different NR–PUAs

Different NR–PUAs were fabricated by adjusting the feed ratios, and the impact of different NR–PUAs was evaluated, as shown in Table 2. As can be seen, with the increase in the feed molar ratios of DMBA to PEG–600 from 5:95 to 30:70, the gel–sol fraction and pencil hardness of the UV coatings decreased from 93.1% to 77.3% and 2 H to H, respectively. Additionally, SD decreased from 1.1227  $\text{g}\cdot\text{mL}^{-1}$  to 1.1175  $\text{g}\cdot\text{mL}^{-1}$ . It can be concluded that the impact of different NR–PUAs on the performance of UV coatings is attributed to the increment in the amount of rigid and steric covalent-grafted NR groups in NR–PUAs.

**Table 2.** Impact of different NR-PUAs on the performance of UV coatings.

Sample	NR-PUA	Molar Ratio of DMBA to PEG-600 in NR-PUAs	Gel-Sol Fraction/wt%	Pencil Hardness	SD/(g·mL <sup>-1</sup> )
Coating-1	NR-PUA-1	5:95	93.1	2H	1.1227
Coating-2	NR-PUA-2	10:90	92.3	2H	1.1221
Coating-3	NR-PUA-3	15:85	89.4	H	1.1192
Coating-4	NR-PUA-4	20:80	83.5	H	1.1189
Coating-5	NR-PUA-5	25:75	77.3	H	1.1175

Conditions: The UV curing time is 50 s. The other conditions are the same as in Table 1.

### 3.1.3. Impact of $n_{\text{acrylate}}:n_{\text{thiol}}$

The impact of  $n_{\text{acrylate}}:n_{\text{thiol}}$  on the performance of the UV coatings is summarized in Table 3. When  $n_{\text{acrylate}}:n_{\text{thiol}}$  was 0.5:1, the gel-sol fraction and the pencil hardness were 85.2 wt% and 1B, respectively. When  $n_{\text{acrylate}}:n_{\text{thiol}}$  was in the range of 1:1–2.5:1, there was almost no change in the gel-sol fraction or the pencil hardness because there was no SD variation in the UV coatings about 1.1189–1.1199 g·mL<sup>-1</sup>.

**Table 3.** Impact of  $n_{\text{acrylate}}:n_{\text{thiol}}$  on the performance of UV coatings.

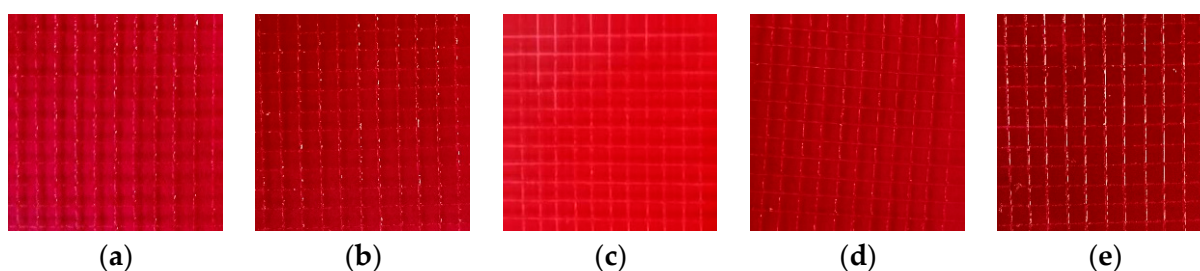
$n_{\text{acrylate}}:n_{\text{thiol}}$	Gel-Sol Fraction/wt%	Pencil Hardness	SD/(g·mL <sup>-1</sup> )
0.5:1	85.2	1 B	1.1187
1:1	89.4	1 H	1.1192
1.5:1	89.1	1 H	1.1199
2.0:1	87.5	1H	1.1189
2.5:1	88.9	1 H	1.1191

Conditions: NR-PUA is NR-PUA-3. The other conditions are the same as in Table 2.

## 3.2. Performance of UV Coatings

### 3.2.1. Adhesive Property

Adhesive performance plays an important role in fields including coatings, electronic device packaging, and sensors, so the adhesive performance of the UV coatings was evaluated. Firstly, the adhesive performance of the UV coatings prepared with different NR-PUAs was explored (Figure 3 and Table 4). When the molar ratio of NP to PEG-600 is in the range of 5:95–25:75, there is almost no shedding area, so the UV coatings have quite good adhesive properties of grade 0 to glass slides.

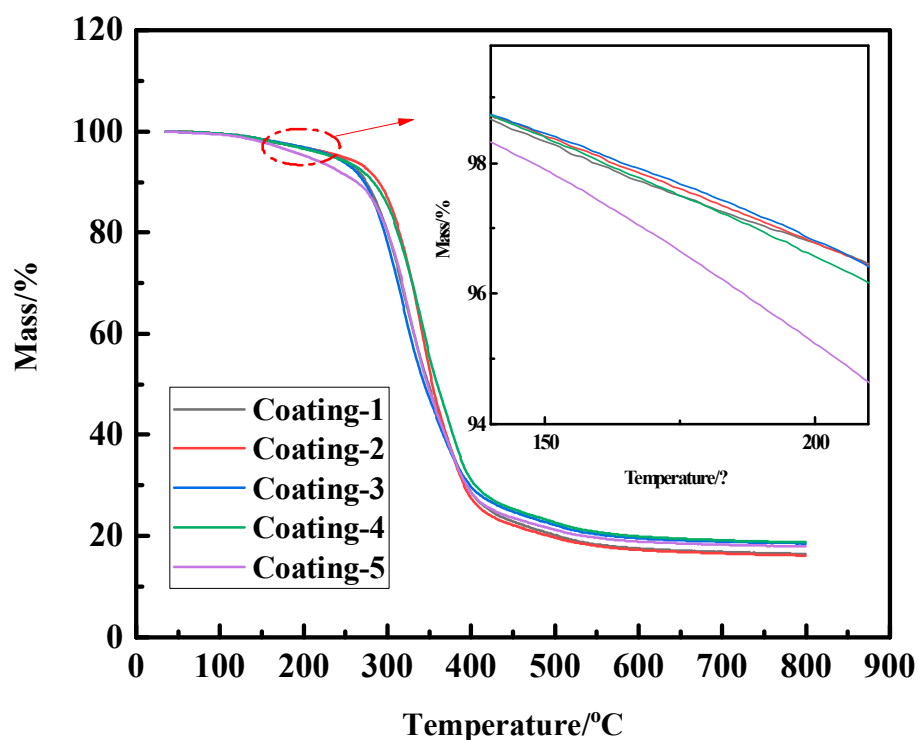
**Figure 3.** Photos of adhesive performance test of UV coatings prepared with different NR-PUAs. (a) Coating-1, (b) Coating-2, (c) Coating-3, (d) Coating-4, and (e) Coating-5.

**Table 4.** The ratio of shedding area and adhesive grade of UV coatings prepared with different NR-PUAs.

	UV Coating-1	UV Coating-2	UV Coating-3	UV Coating-4	UV Coating-5
Ratio of shedding area/%	Almost no shedding area				
Adhesive grade	0	0	0	0	0

### 3.2.2. Thermal Properties

The thermal stability of the UV coatings was evaluated (Figure 4) because it is quite important for coatings and package materials exposed to elevated temperatures. As reported, traditional polyurethanes will undergo severe thermal decomposition at 200 °C [22]. Additionally, the initial thermal decomposition ( $T_{d5}$ ) of pH-sensitive pyranoflavylum–cellulose acetate films fabricated by V. Gomes was also not higher than 200 °C [27]. Compared with those materials reported, the UV coatings exhibited superior thermal stability because the  $T_{d5}$  was in the range of 202–245 °C.

**Figure 4.** TGA curves of UV coatings prepared with different NR-PUAs.

DSC analysis was also adopted to evaluate the thermal performance of the UV coatings. As demonstrated in Figure 5, there was a single glass transition temperature ( $T_g$ ) of the UV coatings, which revealed that the UV coatings were not composites of polymers. The  $T_g$  increased from 8.6 °C to 13.3 °C with the increase in the molar ratio of DMBA to PEG-600 in NR-PUAs from 5:95 to 25:75 because the steric resistance gradually increased thanks to the large NR group.



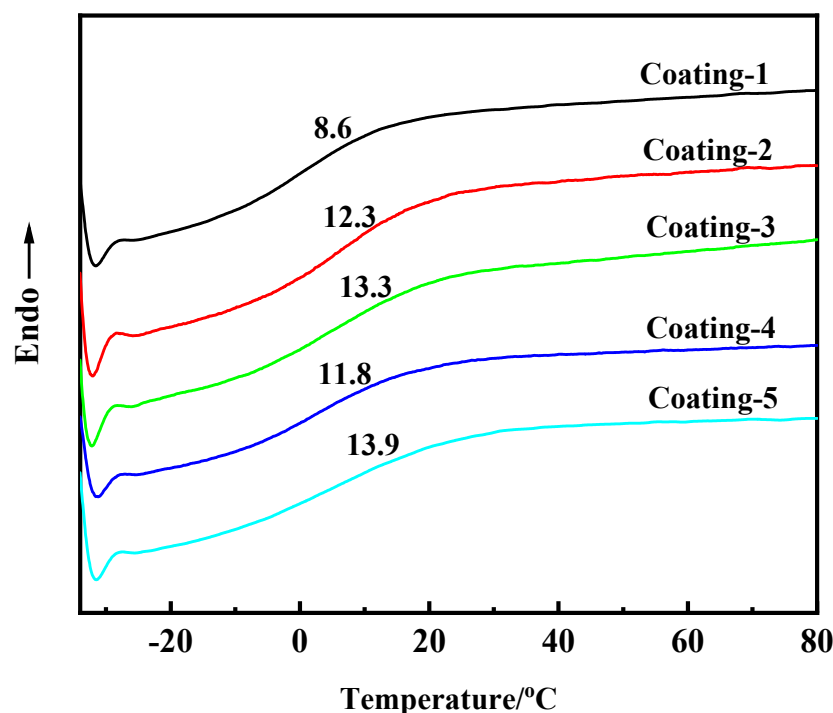


Figure 5. DSC curves of UV coatings prepared with different NR-PUAs.

### 3.2.3. The pH-Sensitive Property

pH-sensitive intelligent materials can serve as sensors in fields including food spoilage [11], chemical reactions [28], specific chemical substance determination [29,30], biotechnology [31,32], biomedical applications [33,34], and monitoring wastewater discharged from chemical industries [35,36]. Therefore, the pH-sensitive performance of the UV coatings was explored (Figure 6). In aqueous solutions with different pH values in the range of 2–12, it can be observed that the color of the UV coatings changed gradually from deep red to yellowish brown. When the pH values were lower than 5, the color was mainly deep red. When the pH values increased from 6 to 12, the color changed from pink to yellowish brown. Thus, the UV coatings have a good pH-sensitive property based on the color change visible to the naked eye. It is well known that the pH-sensitive range of NR is 6.4–8.0 and that the color changes from red to orange [37]. The intelligent pH-sensitive indicator films prepared by the covalent bonding of NR onto cellulose nanofibrils reported by Khanjanzadeh et al. [20] exhibited a visible color variation at a pH value of 2–10. Evidently, the pH-sensitive range of the UV coatings has been obviously expanded.

The covalent bonding of pH indicator groups onto a polymer matrix is a reliable strategy to improve the stability of pH-sensitive intelligent materials. It also can be seen in Figure 6 that the color of the UV coatings no longer changed when they were immersed in an aqueous solution with different pH values for 20 min. Furthermore, the color remained even when the UV coatings were immersed for over 5 h. The pH-sensitive films prepared by Yue et al. exhibited a color change after 30 min of exposure to ammonia with concentrations  $\geq 0.1$  M [9]. Similarly, the intelligent pH-sensitive indicator films reported by Khanjanzadeh et al. [20] also changed from red to yellow after 30 min of exposure to ammonia vapor. Therefore, the UV coatings exhibited considerable variation in pH-sensitivity performance and long-term color stability.

The color variation performance of the UV coatings was also investigated. As exhibited in Figure 7, the distinctive color variation in the UV coatings in different aqueous solutions of different solvents can be observed by the naked eye. This outstanding performance suggests that the UV coatings have the potential to act as sensors for monitoring wastewater with different solvents.

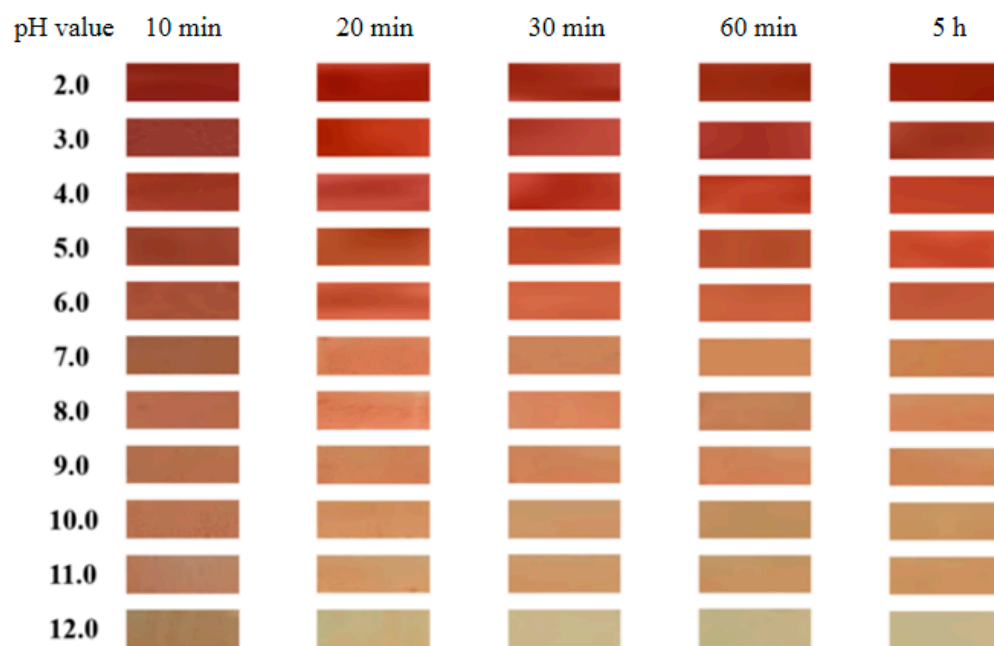


**Figure 6.** Color change in coating-3 immersed in aqueous solutions of different pH values for different times.

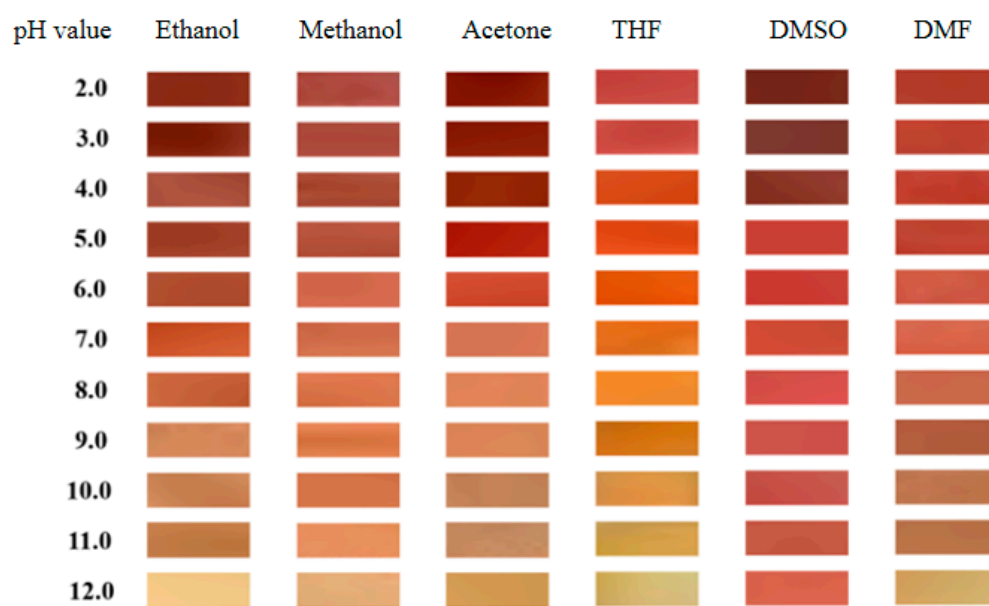
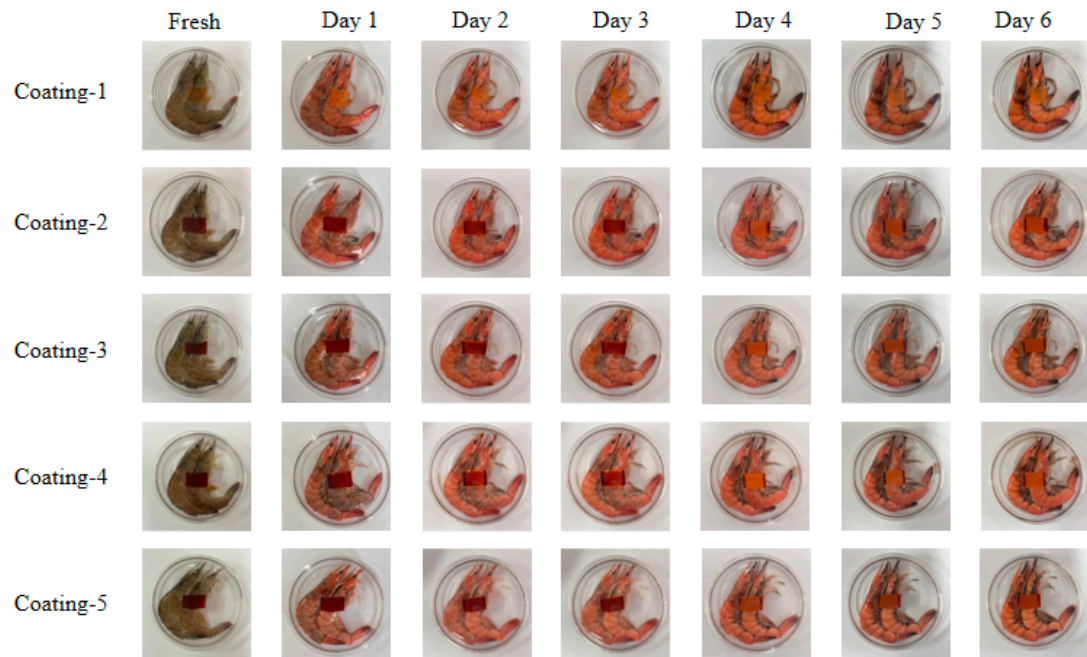


**Figure 7.** Color change in coating-3 immersed in aqueous solutions of different solvents (v:v = 50:50).

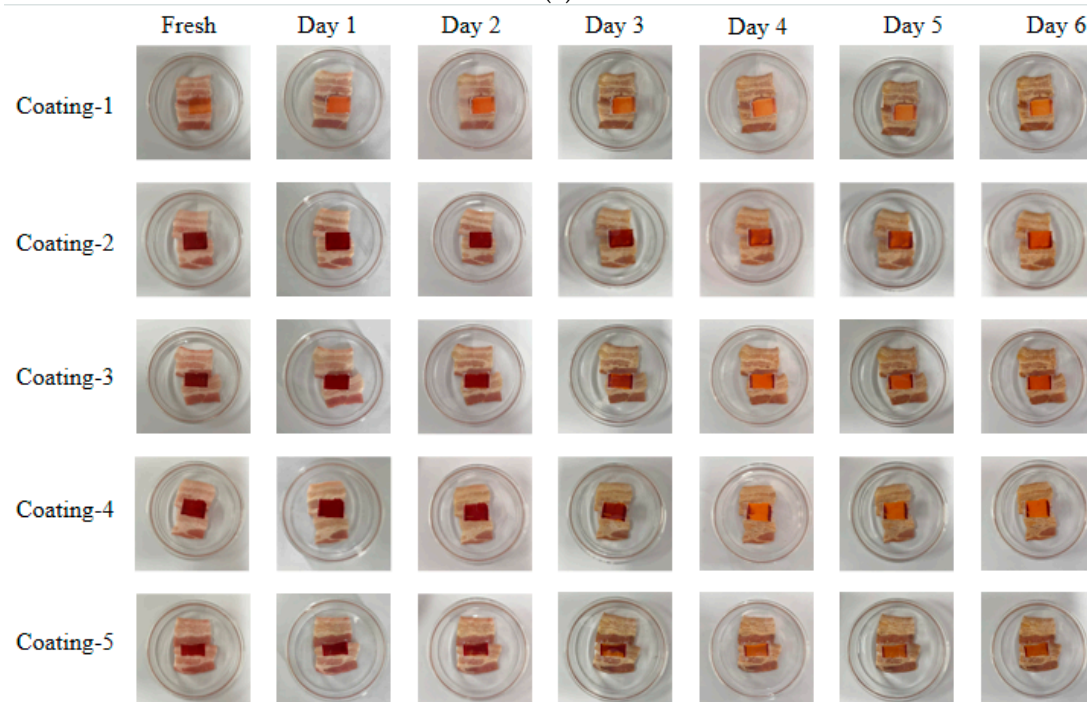
### 3.2.4. Monitoring the Freshness of Shrimp and Pork

During the course of storage and transportation, some high-protein foods such as shrimp and pork deteriorate easily. Eating deteriorated high-protein food by mistake will cause significant harm to health [38,39]. So, it is crucial to develop intelligent materials to monitor food spoilage. If a certain food is contaminated by pathogenic microorganisms, the pH value of the food will change irreversibly because of the metabolite production such as organic acids, CO<sub>2</sub>, and sulfur derivatives [14]. So, color variation in intelligent materials corresponding to pH changes can be adopted to monitor food spoilage [39,40]. As discussed above, the UV coatings exhibited quite good pH-sensitive performance, so an investigation into monitoring spoilage of high-protein food such as shrimp and pork was carried out, as shown in Figure 8. When monitoring the food spoilage of shrimp (Figure 8a),

the color of the pH-sensitive material gradually changed from deep red (fresh) to wine red (day 1), peach red (day 2), light red (day 3), orange-yellow (day 4), and light yellow (day 5 and day 6). Similarly, the color of the pH-sensitive material gradually changed from deep red (Fresh to day 2) to peach red (day 3), orange-yellow (day 4), and light yellow (day 5 and day 6) when the material was applied to monitor the freshness of pork (Figure 8b) So, the pH-sensitive intelligent materials can be used to monitor the food spoilage of shrimp and pork.



(a)



(b)

**Figure 8.** Images taken during the monitoring of the freshness of (a) shrimp and (b) pork.

#### 4. Conclusions

UV-curable, pH-sensitive, intelligent silicone-modified materials for monitoring the freshness of high-protein food such as shrimp and pork were prepared. The materials have good pH-sensitive properties with changes in the color visible to the naked eye and obviously expanded pH values in the range of 2–12. When the pH values were lower than 5, the color was mainly deep red. When the pH values increased from 6 to 12, the color changed from pink to yellowish brown. The materials also exhibited long-term color stability because their color remained even when they were immersed for over 5 h. The distinctive color variation in the UV coatings in different aqueous solutions of different solvents can be observed by the naked eye, which suggests the UV coatings can be used as potential sensors for monitoring wastewater with different solvents. The investigation monitoring the freshness of shrimp and pork revealed that these pH-sensitive intelligent materials can be applied to monitor the freshness of high-protein food. These UV-curable, pH-sensitive, intelligent silicone-modified materials exhibited quite good adhesive properties of grade 0 to glass slides and fairly good thermal stability with  $T_{d5}$  in the range of 202–245 °C. The UV-curable, silicone-modified, pH-sensitive intelligent materials have potential applications in monitoring the freshness of high-protein food such as shrimp and pork.

**Supplementary Materials:** The following are available online at <https://www.mdpi.com/article/10.3390/coatings14060728/s1>, Table S1: Feed ratios for the preparation of PUAs. Table S2: Feed ratios for the preparation of NR-PUAs.

**Author Contributions:** Conceptualization, X.Y.; formal analysis N.H., H.Z., N.S. and S.S.; investigation, N.H., S.S. and L.X.; data curation, N.H. and J.M.; writing—original draft preparation, N.H.; writing—review and editing, X.Y.; project administration, G.L. and X.Y.; funding acquisition, M.L. All authors have read and agreed to the published version of the manuscript.

**Funding:** This research was funded by the “Pioneer” and “Leading Goose” R&D Program of Zhejiang, grant number 2023C01188.

**Data Availability Statement:** Data is contained within the article.

**Conflicts of Interest:** Shaoqing Shi, Libo Xie and Jie Miao are employed by Yuyao Yuandong Chemical Co., Ltd. The funders had no role in the design of the study; in the collection, analyses, or interpretation of data; in the writing of the manuscript; or in the decision to publish the results.

#### References

1. Domínguez, R.; Pateiro, M.; Gagaoua, M.; Barba, F.J.; Zhang, W.G.; Lorenzo, J.M. A comprehensive review on lipid oxidation in meat and meat products. *Antioxidants* **2019**, *8*, 429. [[CrossRef](#)] [[PubMed](#)]
2. Liu, L.M.; Wu, W.N.; Zheng, L.M.; Yu, J.H.; Sun, P.L.; Shao, P. Intelligent packaging films incorporated with anthocyanins-loaded ovalbumin-carboxymethyl cellulose nanocomplexes for food freshness monitoring. *Food Chem.* **2022**, *387*, 132908. [[CrossRef](#)] [[PubMed](#)]
3. Gomes, V.; Bermudez, R.; Mateus, N.; Guedes, A.; Lorenzo, J.M.; de Freitas, V.; Cruz, L. Food smart tag: An innovative dynamic labeling system based on pyranoflavylum-based colorimetric films for real-time monitoring of food freshness. *Food Hydrocoll.* **2023**, *143*, 108914. [[CrossRef](#)]
4. Mai, X.T.; Zhang, X.X.; Wang, W.Z.; Zheng, Y.H.; Wang, D.Y.; Xu, W.M.; Liu, F.; Sun, Z.L. Novel PVA/carboxylated cellulose antimicrobial hydrogel grafted with curcumin and  $\epsilon$ -polylysine for chilled chicken preservation. *Food Chem.* **2023**, *424*, 136345. [[CrossRef](#)] [[PubMed](#)]
5. Shang, Z.Y.; Meng, Q.T.; Tian, D.H.; Wang, Y.; Zhang, Z.X.; Zhang, Z.Q.; Zhang, R. Red-emitting fluorescent probe for hydrogen sulfide detection and its applications in food freshness determination and in vivo bioimaging. *Food Chem.* **2023**, *427*, 136701. [[CrossRef](#)] [[PubMed](#)]
6. Grzebieniarczyk, W.; Tkaczewska, J.; Juszczak, L.; Krzyściak, P.; Cholewa-Wójcik, A.; Nowak, N.; Guzik, P.; Szuwarzyński, M.; Mazur, T.; Jamróz, E. Improving the quality of multi-layer films based on furcellaran by immobilising active ingredients and impact assessment of the use of a new packaging material. *Food Chem.* **2023**, *428*, 136759. [[CrossRef](#)] [[PubMed](#)]
7. Wu, W.N.; Liu, L.M.; Zhou, Y.; Shao, P. Highly ammonia-responsive starch/PVA film with gas absorption system as the ‘bridge’ for visually spoilage monitoring of animal-derived food. *Food Chem.* **2024**, *430*, 137032. [[CrossRef](#)] [[PubMed](#)]

8. Sangeetha, U.K.; Sudhakaran, N.; Parvathy, P.A.; Abraham, M.; Das, S.; De, S.; Sahoo, S.K. Coconut husk-lignin derived carbon dots incorporated carrageenan based functional film for intelligent food packaging. *Int. J. Biol. Macromol.* **2024**, *266*, 131005. [[CrossRef](#)] [[PubMed](#)]
9. Yue, C.Z.; Wang, M.S.; Zhou, Z.L.; You, Y.Z.; Wang, G.Y.; Wu, D.R. Cellulose-based intelligent packaging films with antibacterial, UV-blocking, and biodegradable properties for shrimp freshness monitoring. *Chem. Eng. J.* **2024**, *488*, 150975. [[CrossRef](#)]
10. Ronte, A.; Chalitagkoon, J.; Foster, E.J.; Monvisade, P. Development of a pH-responsive intelligent label using low molecular weight chitosan grafted with phenol red for food packaging applications. *Int. J. Biol. Macromol.* **2024**, *266*, 131212. [[CrossRef](#)]
11. Danchuk, A.I.; Komova, N.S.; Mobarez, S.N.; Doronin, S.Y.; Burmistrova, N.A.; Markin, A.V.; Duerkop, A. Optical sensors for determination of biogenic amines in food. *Anal. Bioanal. Chem.* **2020**, *412*, 4023–4036. [[CrossRef](#)] [[PubMed](#)]
12. Li, B.; Bao, Y.; Li, J.X.; Bi, J.F.; Chen, Q.Q.; Cui, H.J.; Wang, Y.X.; Tian, J.L.; Shu, C.; Wang, Y.H.; et al. A sub-freshness monitoring chitosan/starch-based colorimetric film for improving color recognition accuracy via controlling the pH value of the film-forming solution. *Food Chem.* **2022**, *388*, 132975. [[CrossRef](#)] [[PubMed](#)]
13. Karaca, I.M.; Haskaraca, G.; Ayhan, Z.; Gültekin, E. Development of real time-pH sensitive intelligent indicators for monitoring chicken breast freshness/spoilage using real packaging practices. *Food Res. Int.* **2023**, *173*, 113261. [[CrossRef](#)] [[PubMed](#)]
14. Kong, J.L.; Ge, X.H.; Sun, Y.T.; Mao, M.R.; Yu, H.R.; Chu, R.X.; Wang, Y. Multi-functional pH-sensitive active and intelligent packaging based on highly cross-linked zein for the monitoring of pork freshness. *Food Chem.* **2023**, *404*, 134754. [[CrossRef](#)] [[PubMed](#)]
15. Cao, L.; Sun, G.; Zhang, C.; Liu, W.; Li, J.; Wang, L. An intelligent film based on Cassia gum containing bromothymol blue-anchored cellulose fibers for real-time detection of meat freshness. *J. Agric. Food Chem.* **2019**, *67*, 2066–2074. [[CrossRef](#)]
16. Zia, J.; Mancini, G.; Bustreo, M.; Zych, A.; Donno, R.; Athanassiou, A.; Fragouli, D. Porous pH natural indicators for acidic and basic vapor sensing. *Chem. Eng. J.* **2021**, *403*, 126373. [[CrossRef](#)]
17. Nath, V.A.; Raja, V.; Leena, M.M.; Moses, J.A.; Anandharamakrishnan, C. Co-electrospun-electrosprayed ethyl cellulose-gelatin nanocomposite pH-sensitive membrane for food quality applications. *Food Chem.* **2022**, *394*, 133420. [[CrossRef](#)]
18. Hao, Y.P.; Kang, J.M.; Guo, X.Q.; Sun, M.Y.; Li, H.; Bai, H.T.; Cui, H.X.; Shi, L. pH-responsive chitosan-based film containing oregano essential oil and black rice bran anthocyanin for preserving pork and monitoring freshness. *Food Chem.* **2023**, *403*, 134393. [[CrossRef](#)]
19. Martinez-Haro, M.; Pais-Costa, A.J.; Verdelhos, T.; Marques, J.C.; Acevedo, P. Optimising a clearance index based on neutral red as an indicator of physiological stress for bivalves. *Ecol. Indic.* **2016**, *71*, 514–521. [[CrossRef](#)]
20. Khanjanzadeh, H.; Park, B.-D.; Pirayesh, H. Intelligent pH- and ammonia-sensitive indicator films using neutral red immobilized onto cellulose nanofibrils. *Carbohydr. Polym.* **2022**, *296*, 119910. [[CrossRef](#)]
21. Patil, R.S.; Thomas, J.; Patil, M.; John, J.; Tanski, T.; Wieczorek, A.N.; Staszuk, M. To shed light on the UV curable coating technology: Current state of the art and perspectives. *J. Compos. Sci.* **2023**, *7*, 513. [[CrossRef](#)]
22. Liu, J.L.; Jiao, X.J.; Cheng, F.; Fan, Y.X.; Wu, Y.F.; Yang, X.F. Fabrication and performance of UV cured transparent silicone modified polyurethane-acrylate coatings with high hardness, good thermal stability and adhesion. *Prog. Org. Coat.* **2020**, *144*, 105673. [[CrossRef](#)]
23. Cheng, F.; Fan, Y.X.; He, N.; Song, Y.; Shen, J.B.; Gong, Z.S.; Tong, X.M.; Yang, X.F. Castor oil based high transparent UV cured silicone modified polyurethane acrylate coatings with outstanding tensile strength and good chemical resistance. *Prog. Org. Coat.* **2022**, *163*, 106624. [[CrossRef](#)]
24. Yang, X.F.; Cheng, F.; Fan, Y.X.; Song, Y.; He, N.; Lai, G.Q.; Gong, Z.S.; Shen, J.B. Highly transparent acrylate epoxidized soybean oil based UV-curable silicone-modified coatings with good thermal stability and flame retardancy. *Prog. Org. Coat.* **2022**, *165*, 106769. [[CrossRef](#)]
25. le Gars, M.; Delvart, A.; Roger, P.; Belgacem, M.N.; Bras, J. Amidation of TEMPO-oxidized cellulose nanocrystals using aromatic aminated molecules. *Colloid Polym. Sci.* **2020**, *298*, 603–617. [[CrossRef](#)]
26. Jiao, X.J.; Liu, J.L.; Jin, J.; Cheng, F.; Fan, Y.X.; Zhang, L.; Lai, G.Q.; Hua, X.L.; Yang, X.F. UV cured transparent silicone materials with high tensile strength prepared from hyperbranched silicon-containing polymers and polyurethane-acrylates. *ACS Omega* **2021**, *6*, 2890–2898. [[CrossRef](#)]
27. Gomes, V.; Pires, A.S.; Mateus, N.; de Freitas, V.; Cruz, L. Pyranoflavylum-cellulose acetate films and the glycerol effect towards the development of pH-freshness smart label for food packaging. *Food Hydrocolloid* **2022**, *127*, 107501. [[CrossRef](#)]
28. Martínez-Ruano, J.; Suazo, A.; Véliz, F.; Otálora, F.; Conejeros, R.; González, E.; Aroca, G. Electro-fermentation with *Clostridium autoethanogenum*: Effect of pH and neutral red addition. *Environ. Technol. Innov.* **2023**, *31*, 103183. [[CrossRef](#)]
29. Ghica, M.E.; Pauliukaite, R.; Marchand, N.; Devic, E.; Brett, C.M.A. An improved biosensor for acetaldehyde determination using a bienzymatic strategy at poly(neutral red) modified carbon film electrodes. *Anal. Chim. Acta* **2007**, *591*, 80–86. [[CrossRef](#)]
30. Ericson, M.N.; Shankar, S.K.; Chahine, L.M.; Omary, M.A.; von Herbing, I.H.; Marpu, S.B. Development of neutral red as a pH/pCO<sub>2</sub> luminescent sensor for biological systems. *Chemosensors* **2021**, *9*, 210. [[CrossRef](#)]
31. Mross, S.; Zimmermann, T.; Winkin, N.; Kraft, M.; Vogt, H. Integrated multi-sensor system for parallel in-situ monitoring of cell nutrients, metabolites, cell density and pH in biotechnological processes. *Sens. Actuators B Chem.* **2015**, *236*, 937–946. [[CrossRef](#)]
32. Arafa, A.A.; Nada, A.A.; Ibrahim, A.Y.; Sajkiewicz, P.; Zahran, M.K.; Hakeim, O.A. Preparation and characterization of smart therapeutic pH-sensitive wound dressing from red cabbage extract and chitosan hydrogel. *Int. J. Biol. Macromol.* **2021**, *182*, 1820–1831. [[CrossRef](#)] [[PubMed](#)]

33. Akyol, A.; Baykal, D.; Akdağ, A.; Şensoy, Ö.; Son, Ç.D. A new ratio-metric pH probe, “ThiAKS Green” for live-cell pH measurements. *Photonic Sens.* **2023**, *13*, 230125. [[CrossRef](#)]
34. Son, M.J.; Kim, T.; Lee, S.-W. Facile synthesis of fluorescent mesoporous nanocarriers with pH-sensitive controlled release of naturally derived dieckol. *Colloid Surf. A* **2023**, *657*, 130535. [[CrossRef](#)]
35. Al-Ansari, M.M.; Li, Z.H.; Masood, A.; Rajaselvam, J. Decolourization of azo dye using a batch bioreactor by an indigenous bacterium *Enterobacter aerogenes* ES014 from the waste water dye effluent and toxicity analysis. *Environ. Res.* **2022**, *205*, 112189. [[CrossRef](#)]
36. Elshikh, M.S.; Alarjani, K.M.; Huessien, D.S.; Elnahas, H.A.M.; Esther, A.R. Enhanced biodegradation of chlorpyrifos by *Bacillus cereus* CP6 and *Klebsiella pneumoniae* CP19 from municipal waste water. *Environ. Res.* **2022**, *205*, 112438. [[CrossRef](#)]
37. Manente, S.; Pieri, S.D.; Iero, A.; Rigo, C.; Bragadin, M. A comparison between the responses of neutral red and acridine orange: Acridine orange should be preferential and alternative to neutral red as a dye for the monitoring of contaminants by means of biological sensors. *Anal. Biochem.* **2008**, *383*, 316–319. [[CrossRef](#)]
38. Kan, J.; Liu, J.; Xu, F.F.; Yun, D.W.; Yong, H.M.; Liu, J. Development of pork and shrimp freshness monitoring labels based on starch/polyvinyl alcohol matrices and anthocyanins from 14 plants: A comparative study. *Food Hydrocoll.* **2022**, *124*, 107293. [[CrossRef](#)]
39. Wang, X.J.; Sun, N.N.; Zhu, H.Y.; Yang, Y.N.; Lai, G.Q.; Yang, X.F.  $\kappa$ -Carrageenan-Based flexible antibacterial and pH-Sensitive hydrogels with phenanthroline covalent conjugation groups. *Food Hydrocoll.* **2023**, *145*, 109088. [[CrossRef](#)]
40. Chalitangkoon, J.; Monvisade, P. Synthesis of chitosan-based polymeric dyes as colorimetric pH-sensing materials: Potential for food and biomedical applications. *Carbohydr. Polym.* **2021**, *260*, 117836. [[CrossRef](#)]

**Disclaimer/Publisher’s Note:** The statements, opinions and data contained in all publications are solely those of the individual author(s) and contributor(s) and not of MDPI and/or the editor(s). MDPI and/or the editor(s) disclaim responsibility for any injury to people or property resulting from any ideas, methods, instructions or products referred to in the content.